Controlling of magnetocaloric effect in $Gd_2O_3@SiO_2$ nanocomposites by substrate dimensionality and particles' concentration

Adriana Zeleňáková, Pavol Hrubovčák, Ondrej Kapusta, Anna Berkutova, Vladimir Zeleňák, and Victorino Franco

Citation: AIP Advances **8**, 048105 (2018);
View online: https://doi.org/10.1063/1.4993974
View Table of Contents: http://aip.scitation.org/toc/adv/8/4
Published by the American Institute of Physics

Controlling of magnetocaloric effect in Gd_2O_3@SiO_2 nanocomposites by substrate dimensionality and particles' concentration

Adriana Zeleňáková,[1,a] Pavol Hrubovčák,[1] Ondrej Kapusta,[1]
Anna Berkutova,[1] Vladimir Zeleňák,[2] and Victorino Franco[3]
[1]*Department of Condensed Matter Physics, University of P. J. Šafárik, Park Angelinum 9, 04001, Košice, Slovakia*
[2]*Department of Inorganic Chemistry, University of P.J. Šafárik, Moyzesova 11, 040 01, Košice, Slovakia*
[3]*Department of Condensed Matter Physics, ICMSE-CSIC, Sevilla University, P.O. Box 1065, 41080 Sevilla, Spain*

(Received 3 July 2017; accepted 23 September 2017; published online 24 October 2017)

The magnetocaloric effect (MCE) of hybrid nanostructures consisting of fine gadolinium oxide (Gd_2O_3) nanoparticles with diameter 7 nm and 12 nm loaded into the pores of the periodically ordered mesoporous silica with hexagonal (SBA-15) or cubic (SBA-16) symmetry were investigated. The concentration effect of the added nanoparticles (NPs) and the effect of the silica matrix dimensionality on the structural properties, magnetization *M(H)*, magnetic entropy change ΔS_M, and parameters *A(T)* and *B(T)* derived from Arrott plots were studied in four samples. Examined nanocomposites exhibited reasonable high values of magnetic entropy change ΔS_M varying from 29 J/kgK established for Gd_2O_3@SBA-15 up to 64 J/kgK observed in Gd_2O_3@SBA-16 at maximal field change 5 T at low temperatures. This suggests that studied nanocomposites, where diamagnetic silica matrices serve as nanoreactors for growth of Gd_2O_3 nanoparticles and their symmetry strongly affect magnetic properties of whole composites, could be feasible for cryomagnetic refrigeration applications. https://doi.org/10.1063/1.4993974

I. INTRODUCTION

The magnetocaloric effect (MCE) refers to conversion of magnetic energy of a magnetic substance into thermal energy under applying or removing an external magnetic field.[1] In the process of tailoring the qualities of potential refrigerants, magnetic nanoparticles have been found very promising.[2] The main advantage of nanoparticles over the bulk materials stems in wider options for tuning the characteristics of the refrigerant material. Since the change of working temperature, refrigeration capacity or phase transition character in bulk materials can be induced almost exclusively by chemical composition, in the case of NPs size, shape, capping layer or dilution of nanoparticle system affects those qualities.[3–5] Based on the calculation of superparamagnetic theory was predicted[6] that nanomagnets would have a larger magnetic entropy change because of the existence of a large magnetic-moment density in a single magnetic particle. Therefore, for the nanoparticles with large atomic moments and low energy barriers, the magnetic moments may easily overcome the barriers to change their alignments to acquire the large entropy change at low temperatures. Several compounds, particularly those based on gadolinium, currently attract attention because of the discovery of their new properties contributing to significant enhancement of MCE.[6,7] Zeng et. al.[8] presented a work in which magnetocaloric properties of the as-consolidated nanocrystalline and coarse-grained

[a]Corresponding author, Electronic mail: adriana.zelenakova@upjs.sk

gadolinium metals were studied. With the decrease of Gd grains from micrometer to nanometer range, magnetic entropy change value exhibited abrupt drop from 10 to 4.47 J/kgK at the same experimental conditions. The effects of nanocrystalline structures on magnetocaloric effect were studied also by Pekala at al[9,10] in various manganite composites. They show that a reduction of crystallite sizes during the transition from a poly-to a nanocrystalline composite causes a suppression of magnetic entropy change, which is accompanied by a considerable broadening of the temperature interval when compared to the polycrystalline material. Therefore, the relative cooling power (RCP(S)) of the nanocrystalline composite is reduced by 10% in comparison with polycrystalline phase. This confirms that the magnetocaloric materials with the more competitive properties may be developed in a form of nanocrystalline composites.[9,10]

Magnetic nanocomposite materials based on magnetic nanoparticles embedded in ordered porous silica matrices have found applications in the various scopes like catalysis, adsorption, chromatography, chemical sensors or biomedicine.[11,12] These composites exhibit the benefits originating from the suitable combination of the features inherent to each fundamental component, like high specific surface area, tunable pore size and volume, high chemical, thermal and mechanical stability or the low toxicity. Several works confirming that embedding of nanostructures into matrix material could result in feasible effects with respect to thermal conductivity of the composite have been published. Zhang et al.[13] showed that it is possible to affect thermal conductivity of nanocomposite by tailoring nanoparticles' size distribution in order to scatter in broader or narrower thermal phonon spectrum. According to simulations carried out by Quiao et al.,[14] for nanocomposite with randomly dispersed nanoparticles, thermal conductivity of matrix material can be enhanced by embedding nanoparticles exhibiting high thermal conductivity. Thus, properly designed nanocomposite which would combine feasible features like high value of magnetic entropy change along with good thermal stability and conductivity could exhibit suitable properties with respect to magnetocaloric applications.

With the aim to confirm the direct influence of silica matrix symmetry (2D or 3D) and nanoparticles' concentration on the magnetocaloric response, we performed the study of nanocomposites containing gadolinium oxide nanoparticles (Gd_2O_3) loaded into the mesoporous silica matrix. The method of nanocasting was employed for the samples' preparation. Mesoporous silica matrices of two different kinds of symmetry served as hard templates for growth of the nanoparticles.[11,12] High values of magnetic entropy change and refrigeration capacity were observed at low temperatures. Mutual comparison of the results obtained from all of the samples revealed the variance in their magnetic and magnetocaloric characteristics, what suggests that these qualities can be controlled by Gd_2O_3 nanoparticles' concentration as well as by the symmetry of silica matrix. The analysis of parameters *A(T)* and *B(T)* derived from Arrott plots revealed the presence of the second order phase transition in studied nanocomposites. Our finding along with the benefits of mesoporous nanocomposite could extend the current Gd_2O_3 NPs applications to the area of cryogenic refrigeration, e.g., as a material for Nano Electro Mechanical Systems (NEMS).

II. EXPERIMENTAL

Nanocomposite samples consisting of Gd_2O_3 nanoparticles encapsulated into silica matrix with 2D organization of mesopores (hexagonal symmetry) and with 3D ordering of pores (cubic symmetry) were prepared by nanocasting method. At first, a blank mesoporous silica matrix SBA-15 (hexagonal) and SBA-16 (cubic) were synthesized according to Zhao, et al.[15] and Kim et al.,[16] respectively. Subsequently, the blank matrices were used as a hard template and they were modified by gadolinium oxides via wet-impregnation. In the typical experiment, the 1 g of dehydrated samples SBA-15 or SBA-16, were wet-impregnated with 20 ml of 0.5 M and 4 M solutions of $Gd(NO_3)_3$ for 2 h at room temperature. After the impregnation the samples were being dried at 323 K for 2 h. The dry material was heated by the rate 1 K/min up to the target temperature 773 K. The four prepared samples with different nanoparticle concentrations were denoted as **Gd_2O_3@SBA-15 low** for low NPs concentration and hexagonal matrix symmetry, **Gd_2O_3@SBA-15 high** for high NPs concentration and hexagonal matrix symmetry, **Gd_2O_3@SBA-16 low** for low NPs concentration and cubic matrix symmetry and **Gd_2O_3@SBA-16 high** for high NPs concentration and cubic matrix symmetry.

The HRTEM (high-resolution transmission electron microscopy) micrographs were taken with JEOL 2100F microscope. Copper grid coated with a holey carbon support was used to prepare samples for the TEM observation. The bright-field TEM image was obtained at 200 kV. EDX (energy-dispersive X-ray spectroscopy) measurement performed by TEM confirmed the presence of Gd_2O_3.[17]

X-ray powder diffraction was used for phase analysis of nanoparticles inside porous matrices. Diffraction measurements were carried out by synchrotron radiation with energy 60 kV and wavelength λ = 0.0207 nm on accelerator PETRA III in DESY, Hamburg. Samples were put into Capton capillaries. Diffraction patterns were integrated and processed via FIT2D software and CeO_2 was used as calibration standard. The scattering intensity was measured as a function of scattering vector, q, being defined as $q = (4\pi/\lambda)\sin\theta$, where 2θ is the scattering angle and λ is the X-ray wavelength.

The filling process of nanocomposites was N_2 sorption/desorption experiments. The textural properties of the parent silica matrices and their nanocomposites were performed with a Quantachrome Gas Sorption System at 77 K. The specific surface area, SBET, was estimated using Brunauer–Emmett–Teller (BET) equation in the relative pressure range (0.05–0.30). Pore volumes and pore size distribution were calculated using the NLDFT theory for cylindrical pores (SBA-15) or spherical pores (SBA-16). In addition, to determine of the quantity of the gadolinium oxide in the samples, the samples were dissolved in the hydrofluoric acid and the gadolinium content was analyzed by atomic absorption spectroscopy (AAS). The determined content of gadolinium corresponded to the 10wt. % in the samples **Gd_2O_3@SBA-15 low** and **Gd_2O_3@SBA-16 low** and 25wt.% in the samples **Gd_2O_3@SBA-15 high** and **Gd_2O_3@SBA-16 high.**

Magnetic properties of the composites were investigated using commercial MPMS 5XL and MPMS 3 (Quantum Design) devices. The dependences of magnetization on field magnitude (up to 5 T) were recorded in temperature range 2 – 52 K with the step of 1 K. The powder samples were encapsulated into a gelatin capsule and inserted into the plastic sample holder. The signals of diamagnetic contributions of gelatin capsule and plastic sample holder were measured and subtracted from experimental data. Experimental isothermal magnetization data were processed employing Maxwell thermodynamic relation and Matlab software in order to calculate the dependence of magnetic entropy change on temperature of the investigated material.

III. RESULTS AND DISCUSSION

The periodic organization of the hexagonal and cubic nanocomposites was confirmed by HRTEM micrographs in all studied samples. Figs. 1a) and 2a) show schematically the arrangement of Gd_2O_3 NPs inside SBA-15 (hexagonal) and SBA-16 (cubic) silica matrix. The HRTEM micrographs of nanocomposite with hexagonal symmetry with low (Fig. 1b)) and high (Fig. 1c)) Gd_2O_3 nanoparticle concentration show on gradual increase in porous system filling and on the fact that regular porous architecture retained its periodicity after nanocasting by NPs. In both hexagonal nanocomposites (**Gd_2O_3@SBA-15 low** and **Gd_2O_3@SBA-15 high**), the size of pores around 8 nm was estimated from HRTEM. Similar periodic cubic arrangement of nanocomposites was observed after

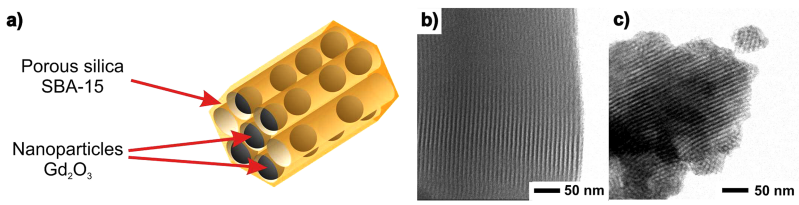

FIG. 1. Structure of magnetic nanocomposite with hexagonal symmetry. a) Schema of Gd_2O_3 nanoparticles embedded in SiO_2 matrix with hexagonal symmetry, b) TEM picture of **Gd_2O_3@SBA-15 low** with low concentration of NPs, c) TEM picture of **Gd_2O_3@SBA-15 high** with high concentration of NP. The views with parallel orientation of the longitudinal hexagonal axis to the surface of the composite.

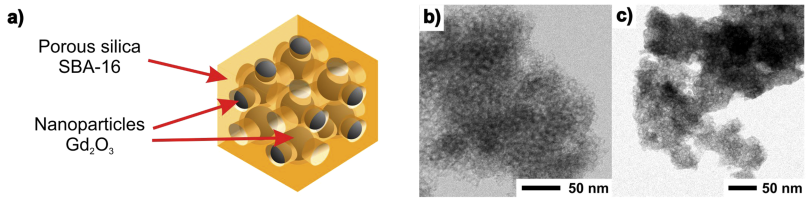

FIG. 2. Structure of magnetic nanocomposite with cubic symmetry. a) Schema of Gd_2O_3 nanoparticles embedded in SiO_2 matrix with cubic symmetry, b) TEM picture of **Gd_2O_3@SBA-16 low** with low concentration of NPs, c) TEM picture of **Gd_2O_3@SBA-16 high** with high concentration of NPs.

embedding of Gd_2O_3 in SBA-16 silica, Figs. 2b), 2c). The cell parameters of cubic nanocomposites (**Gd_2O_3@SBA-16 low** and **Gd_2O_3@SBA-16 high**) as estimated from HRTEM micrographs, is about 16 nm, what is in good agreement with the value calculated from SAXS data for blank SBA-16.[18]

Further structural characterization was performed by high energy X-ray diffraction (HE-XRD) measurements using synchrotron radiation. XRD spectra document the presence of amorphous silica and gadolinium oxides of Gd_2O_3 type in all modified samples. The representative spectra of studied nanocomposites are presented in Fig. 3. The large full width at half maximum of diffraction peaks recognized in the patterns indicates the nanocrystalline character of the particles. All four samples exhibited broad peaks at around 2θ = 3.98° and 2θ = 6.2°, assigned to amorphous silica,[19] which overlap almost whole diffraction peaks from gadolinium oxide nanoparticles. In spite of this, there is still clear evidence of Gd_2O_3 presence in the XRD spectra of nanoparticles in porous silica matrix

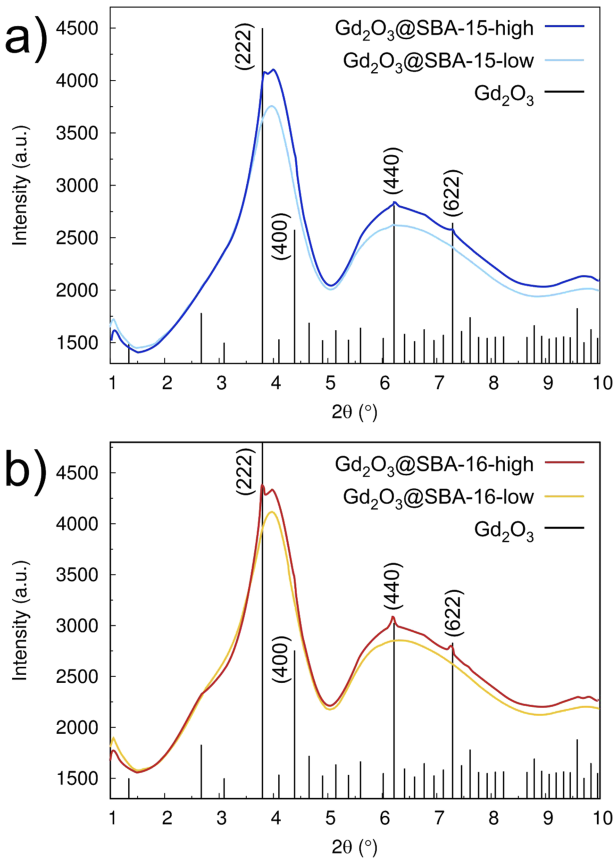

FIG. 3. Diffraction pattern of studied samples a) **Gd_2O_3@SBA-15 low** (light blue line) and **Gd_2O_3@SBA-15 high** (dark blue line) with hexagonal matrix symmetry, b) **Gd_2O_3@SBA-16 low** orange line) and **Gd_2O_3@SBA-16 high** (red line) with cubic matrix symmetry. The solid lines represent the peak positions of the gadolinium oxide reference (JCPDS No. 43–1014).

(space group *Ia-3* (No. 206), JCPDS No. 43-1014), with major diffraction peaks at 2θ values 3.84°, 4.43°, 6.25°, 7.33°, corresponding to (2 2 2), (4 0 0), (4 4 0) and (6 2 2) reflections. Overlapping of diffraction peaks from amorphous silica and gadolinium oxide nanoparticles also suggests on the sufficient encapsulation of the NPs inside internal porous system. With increasing particles concentration, the intensity of Gd_2O_3 signal rises, what is in agreement with results from HRTEM and N_2 sorption/desorption method.[18]

Figs. 4 a) – d) present the isothermal magnetization $M(\mu_0 H)$ data of investigated material measured in temperature range 2 – 52 K with the step of 1 K. The curves recorded at lowest temperatures resemble "S" shape, while the tendency of becoming almost linear with increasing temperature is evident in all studied samples. This behavior is expected for paramagnetic or superparamagnetic materials.[2] With increasing concentration of Gd_2O_3 NPs in nanocomposite with hexagonal symmetry, Figs. 4 a), b), the magnetization measured at corresponding temperatures is gradually enhanced, what confirms the successive filling process of porous matrix system by nanoparticles. On the contrary, in nanocomposites with cubic symmetry, the magnetization increases up to critical nanoparticle concentration (it was observed in our previous studies) and beyond this "limit", the magnetization decreases. In Figs. 4 c), d) can be seen *M(H)* curves recorded in nanocomposite with cubic symmetry below critical concentration limit, represented by higher magnetization values, Fig. 4c), and beyond this critical limit showing lower magnetization values, see Fig. 4 d). This confirms that with gradually increasing nanoparticle concentration in cubic nanocomposites, the certain fraction of Gd_2O_3 is evicted out from internal surface pores. $M(\mu_0 H)$ data displayed in Fig. 4 were processed for the evaluation of magnetocaloric properties of the material.

Magnetic entropy change (ΔS_M) calculations were carried out employing Maxwell relation $(\partial M/\partial T)_H = (\partial S/\partial H)_T$ expressing how change in magnetization induces magnetic entropy change, and vice versa. Thus, in the case of isothermal-isobaric process after integration we get magnetic entropy change[20]

$$\Delta S_M = \int \left(\frac{\partial M}{\partial T}\right)_H dH \tag{1}$$

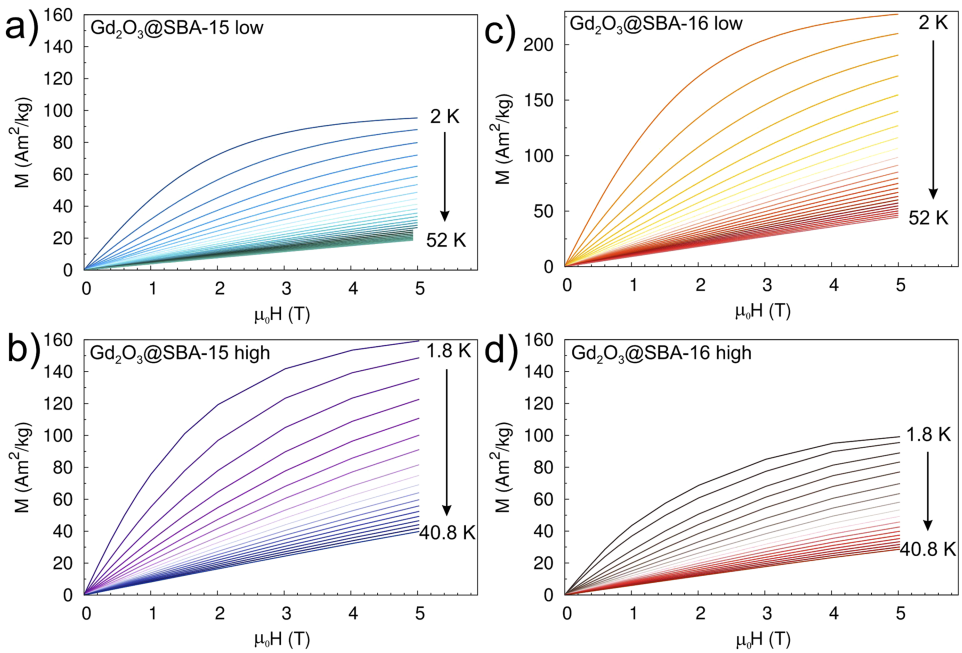

FIG. 4. Isothermal magnetization data of Gd_2O_3@SiO_2 nanocomposites up to applied field of 5 T obtained in temperature range 2 – 52 K with the step 1 K. a) Sample **Gd_2O_3@SBA-15 low** with hexagonal symmetry of silica matrix and low concentration of NPs, b) sample **Gd_2O_3@SBA-15 high** with hexagonal symmetry of silica matrix and high concentration of NPs, c) sample **Gd_2O_3@SBA-16 low** with cubic symmetry of silica matrix and low concentration of NPs and, d) sample **Gd_2O_3@SBA-16 high** with cubic symmetry of silica matrix and high concentration of NPs.

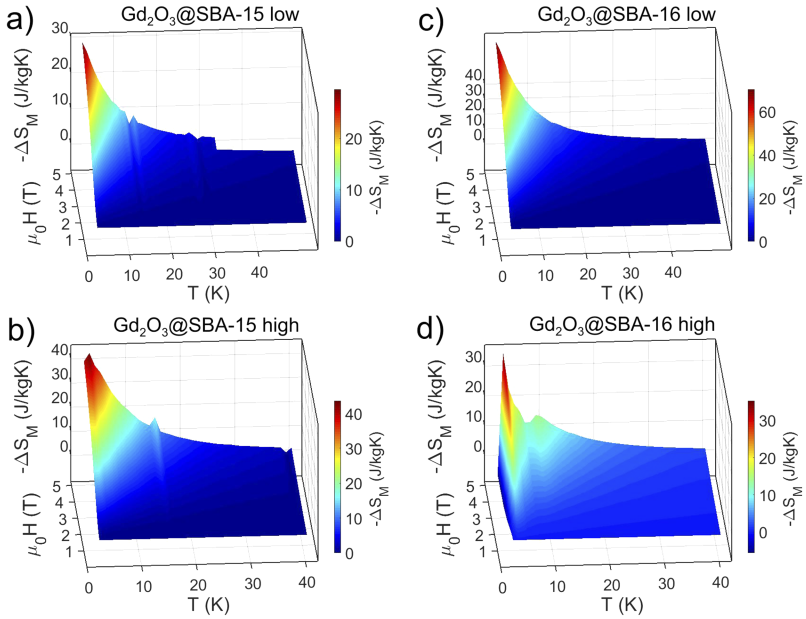

FIG. 5. Magnetic entropy change vs. temperature dependences of whole composites Gd_2O_3@SiO_2. a) Sample **Gd_2O_3@SBA-15 low,** b) sample **Gd_2O_3@SBA-15 high**, c) sample **Gd_2O_3@SBA-16 low** and, d) sample **Gd_2O_3@SBA-16 high**.

For the discrete measurements, there is a numerical approximation of the Eq. (1)[21,22]

$$\Delta S_M\left(\frac{T_{n+1}+T_n}{2}, \mu_0 H\right) = \sum \frac{(M_{n+1}-M_n)_{\mu_0 H}}{T_{n+1}-T_n}\Delta\mu_0 H, \tag{2}$$

where M_n and M_{n+1} are the magnetization values measured in magnetic field $\mu_0 H$ at temperatures T_n and T_{n+1}, respectively. Fig. 5 shows the temperature dependences of magnetic entropy change $\Delta S_M(T)$ at different magnetic field variations (up to 5 T) calculated from experimental data displayed in Fig. 4 for all studied nanocomposites. At higher temperature region, slight increase of ΔS_M with decreasing temperature can be seen.

Gradual enhancement of $-\Delta S_M$ with the increase of magnetic field change is also evident for all the samples in the Fig. 5. Approaching to the lowest temperatures, $-\Delta S_M$ soars while reaching the maximal values of 29 J/kgK at 2 K for the sample **Gd_2O_3@SBA-15 low**, $\Delta S_M(T) = 43$ J/kgK at 3 K for **Gd_2O_3@SBA-15 high**, $\Delta S_M(T) = 64$ J/kgK at 2 K for **Gd_2O_3@SBA-16 low**, and $\Delta S_M(T) = 38$ J/kgK at 3 K for **Gd_2O_3@SBA-16 high** for field variation 5 T. These large values of $\Delta S_M(T)$ observed in all studied samples are much higher than the values reported for conventional superparamagnetic nanoparticles[23] and they are comparable with $GdAl_2$@Al_2O_3 nanocapsules,[21] where $\Delta S_M(T)$ can reach the largest values of 18.02, 18.71, and 31.01 J/kgK at 7.5 K for field variation from 1-7 T, and oxalate-bridged Gd(III) coordination polymers[24] with $\Delta S_M(T)$ = 32.9 J/kgK at 2.6 K for field variation 1-7 T.

Neither the MCE nor such a high value of magnetic entropy change have ever been measured and detected in Gd_2O_3@SiO_2 nanocomposites. Further investigation of magnetic properties and the determination of magnetic transition type was performed employing well established Arrott plot analysis.[9,10,25,26] The plots were constructed from the isothermal magnetization data as a function of magnetic field from 0 to 5 T for each corresponding sample, Fig. 6.

According to the Banerjee criterion, the positive slope of $\mu_0 H/M$ vs. M^2 at very low temperatures suggests on the second order magnetic phase transition.[25–28] According to Landau theory, a theoretical modeling of the MCE could also provide the proof of characteristics typical of magnetic transition. The Gibbs free energy can be expressed as[25]

$$G(T,M) = G_0 + \frac{1}{2}A(T)M^2 + \frac{1}{4}B(T)M^4 - \mu_0 HM, \tag{3}$$

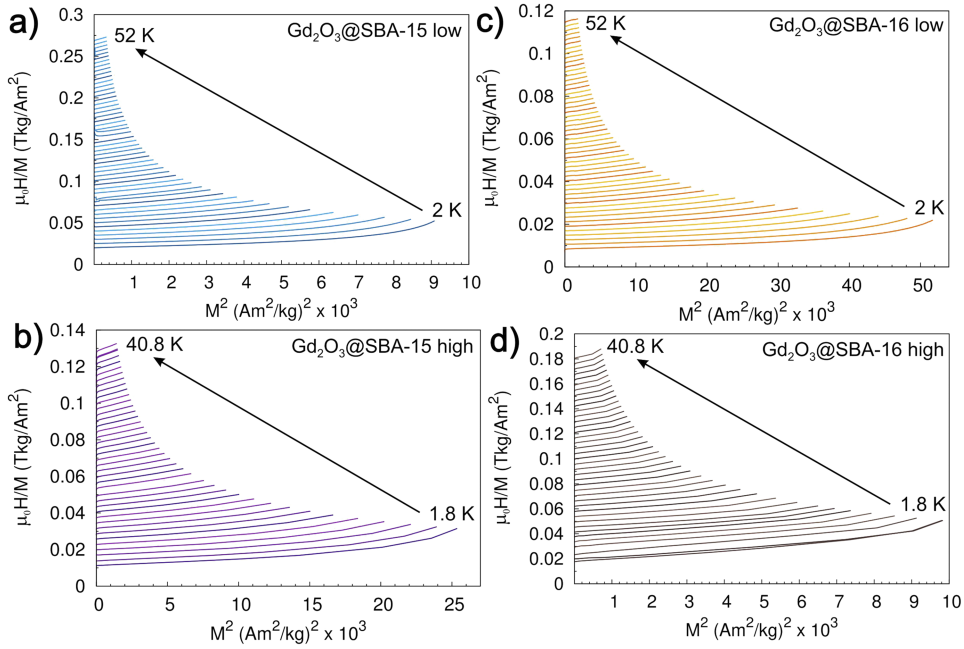

FIG. 6. Standard Arrott plots (isotherms $\mu_0 H/M$ vs. M^2) around critical temperature. a) Sample **Gd_2O_3@SBA-15 low,** b) sample **Gd_2O_3@SBA-15 high**, c) sample **Gd_2O_3@SBA-16 low** and, d) sample **Gd_2O_3@SBA-16 high**.

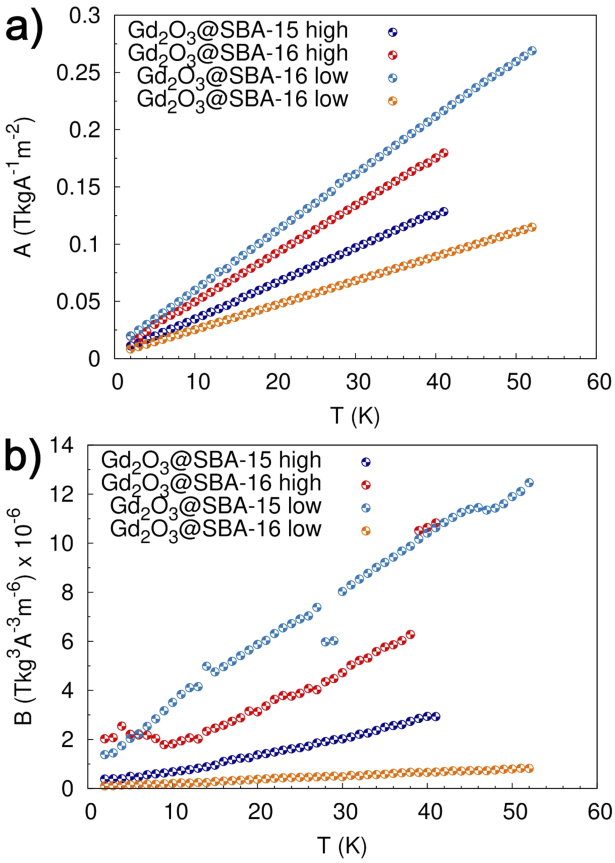

FIG. 7. Temperature dependence of the parameters *A(T)* and *B(T)* of studied nanocomposites.

where *A(T)* and *B(T)* parameters are temperature dependent representing the electron condensation energy and magnetoelastic coupling. Assuming the condition of equilibrium we obtain[26]

$$\frac{\mu_0 H}{M} = A(T) + B(T)M^2. \tag{4}$$

The parameters *A(T)* and *B(T)* obtained from the linear region of the Arrott plots are shown in the Fig. 7.

One can clearly find that the parameter *A(T)* increases with increasing temperature. If we consider our previous results, the critical temperature of samples with higher concentration of NPs (**Gd_2O_3@SBA-15 high** and **Gd_2O_3@SBA-16 high**) was established at T_{max} = 3 K, thus the existence the second order phase transition (SOPT) in measured temperature interval 1.8-41 K was confirmed. Despite of no evidence of $\Delta S_M(T)$ peaks in nanocomposites with low nanoparticle concentration, the positive[27,28] parameter *B(T)* at very low temperatures might suggest the presence of the second order phase transition in all studied nanocomposites.

IV. CONCLUSION

To summarize, we have studied the structural, magnetic and magnetocaloric properties of Gd_2O_3@SiO_2 nanocomposite prepared by nanocasting of Gd_2O_3 nanoparticles of two different concentrations in periodic nanoporous silica matrix with hexagonal (SBA-15) and cubic symmetry (SBA-16). The concentration effect of the added nanoparticles (NPs) and the effect of the matrix dimensionality on the structural properties, magnetization *M(H)*, magnetic entropy change ΔS_M and parameters *A(T)* and *B(T)* from Arrott plots were studied. Mutual comparison of the results obtained from all of the samples revealed the variance in their magnetic and magnetocaloric characteristics, what suggests that these qualities can be tuned rather easily. Our finding along with the benefits of mesoporous nanocomposites could extend the current Gd_2O_3 nanoparticle applications and bring the new insight into the application of such kind of materials in cryomagnetic refrigeration.

ACKNOWLEDGMENTS

This work was supported by the Slovak Research and Development Agency under the contracts APVV-15-0520, APVV-14-0073 and APVV-15-0115, and by the VEGA projects No. 1/0745/17, No. 1/0377/16.

[1] A. M. Tishin and Y. I. Spichkin, *The Magnetocaloric Effect and its Applications* (CRC Press, Boca Raton, 2003).
[2] M. H. Phan, M. B. Morales, C. N. Chinnasamy, B. Latha, V. G. Harris, and H. Srikanth, J. Phys. D: Appl. Phys. **42**, 115007 (2009).
[3] P. Poddar, S. Srinath, J. Gass, B. L. V. Prasad, and H. Srikanth, J. Phys.Chem. C **111**, 14060 (2007).
[4] P. Poddar, J. Gass, D. J. Rebar, S. Srinath, H. Srikanth, S. A. Morrison, and E. E. Carpenter, J. Magn. Magn. Mater. **307**, 227 (2006).
[5] V. Franco and A. Conde, Scr. Mater. **67**, 594 (2012).
[6] S. Ma, W. F. Li, D. Li, D. K. Xiong, N. K. Sun, D. Y. Geng, W. Liu, and Z. D. Zhang, Phys. Rev. B **76**, 144404 (2007).
[7] Y. Meng, Y. Chen, Z. Zhang, Z. Lin, and M. Tong, Inorg. Chem. **53**, 9052 (2014).
[8] H. Zeng, J. Zhang, C. Kuang, and M. Yue, Appl. Nanosci. **1**, 51 (2011).
[9] M. Pekała, K. Pekała, V. Drozd, K. Staszkiewicz, J.-F. Fagnard, and P. Vanderbemden, J. Appl. Phys. **112**, 023906 (2012).
[10] M. Pękała, K. Pękała, V. Drozd, J.-F. Fagnard, and P. Vanderbemden, Journal of Alloys and Compounds **629**, 98 (2015).
[11] M. Tadic, N. Citakovic, M. Panjan, B. Stanojevic, D. Markovic, D. Jovanovic, and V. Spasojevic, J. Alloy Compd. **543**, 118 (2012).
[12] A. Zelenakova, J. Kovac, and V. Zelenak, J. Appl. Phys. **108**, 034323 (2010).
[13] H. Zhang and A. Minnich, Scientific Reports **5**, 8995 (2015).
[14] R. Quiao and P. He, Molecular Simulation **33**, 677 (2007).
[15] D. Zhao, Q. Huo, J. Feng, B. F. Chmelka, and G. D. Stucky, J. Am. Chem.Soc. **120**, 6024 (1998).
[16] T. W. Kim, R. Ryoo, M. Kruk, K. P. Gierszal, M. Jaroniec, S. Kamiya, and O. Teresaki, J. Phys. Chem. B **108**, 11480 (2004).
[17] A. Zelenakova, P. Hrubovčák, O. Kapusta, A. Berkutova, V. Zeleňák, and V. Franco, Appl. Phys. Lett. **109**, 122412 (2016).
[18] V. Zeleňák, D. Halamová, A. Zeleňáková, and V. Girman, J. Porous Mater. **23**, 1633 (2016).
[19] Q. Huo, D. I. Margolese, and G. D. Stucky, Chem. Mater. **8**, 147 (1996).
[20] V. K. Pecharsky and K. A. Gschneidner, Jr., Phys. Rev. Lett. **78**, 4494 (1997).
[21] S. Ma, W. F. Li, D. Li, D. K. Xiong, N. K. Sun, D. Y. Geng, W. Liu, and Z. D. Zhang, Phys. Rev. B **76**, 144404 (2007).
[22] V. Franco, K. R. Pirota, V. M. Prida, A. M. J. C. Neto, A. Conde, M. Knobel, B. Hernando, and M. Vazquez, Phys. Rev. B **77**, 104434 (2008).

[23] D. Baldomir, J. Rivas, D. Serantes, M. Pereiro, J. E. Arias, M. C. Bujan-Nunez, and C. Vazquez-Vazquez, J. Non-Cryst. Solids **353**, 790 (2007).
[24] Y. Meng, Y. Chen, Z. Zhang, Z. Lin, and M. Tong, Inorg. Chem. **53**, 9052 (2014).
[25] X. Sia, K. Zhou, R. Zhang, Y. Liu, and J. Qi, Physics Letters A **381**, 1693 (2017).
[26] X. Chen and Y. Zhuang, Solid State Communications **260**, 23 (2017).
[27] X. Si, Y. Liu, X. Lu, W. Wang, W. Lei, J. Lin, T. Zhou, and Y. Xu, J. Appl. Phys. **119**, 215104 (2016).
[28] V. S. Amaral, J. P. Araújo, Yu. G. Pogorelov, P. B. Tavares, J. B. Sousa, and J. M. Vieira, J. Magn. Magn. Mater. **242**, 655 (2002).